CRYSTALLIZATION BEHAVIOR, MECHANICAL, MORPHOLOGICAL AND PHYSICAL PROPERTIES OF POLY(BUTELENE SUCCINATE)/HOLLOW GLASS MICROSPHERE COMPOSITES: PARTICLE SIZE AND DENSITY EFFECTS OBSERVATIONS

Nawadon Petchwattana[1], Phisut Naknaen[2], Borwon Narupai[3]

[1] *Division of Polymer Materials Technology*
Faculty of Agricultural Product Innovation and Technology
Srinakharinwirot University, Ongkharak, Nakhon Nayok 26120, Thailand
E-mail: nawadon@g.swu.ac.th
[2] *Division of Food Science and Nutrition*
Faculty of Agricultural Product Innovation and Technology
Srinakharinwirot University, Ongkharak, Nakhon Nayok 26120, Thailand
[3] *Expert Center of Innovative Materials*
Thailand Institute of Scientific and Technological Research
Pathumthani 12120, Thailand

Received 15 October 2018
Accepted 30 September 2019

ABSTRACT

In this paper, poly(butylene succinate) (PBS)/hollow glass microsphere (HGM) composites were prepared with three HGM - K25, S60 and S15. The true density of K25, S60 and S15 were 0.248, 0.604, 0.153 g cm^{-3}, while their average particle size (D50) were 55, 30, 55 μm, respectively. PBS/HGM composites were prepared by a twin screw extruder and an injection molding machine. The melting and crystallization behaviors, mechanical properties, as well as morphology were investigated. Thermal and crystallization behavior test results indicated that the degree of crystallinity of PBS increased by at least 1.7 times with the addition of HGM at all types. Microscopic observation indicated some agglomerations and the pulled-out HGM particles. These restricted the HGM-polymer matrix stress transfer and reduced the tensile strength of the composites. Moreover, some broken HGM particles were clearly observed at 7.5 and 10 wt. %, especially for the HGM with K25 and S15. The density of the PBS/HGM composites were all reduced with the concentration. Minimum density reduction by 17 % was observed when S60 was applied at 10 wt. %.

Keywords: biodegradable polymers, hollow glass microsphere, crystallization behavior, mechanical properties, polymer composites.

INTRODUCTION

Poly(butylene succinate) (PBS) is one of biodegradable polymers, which has drawn much attention due to its interesting properties such as high ductility, commercial availability and biodegradability [1 - 4]. However, its low strength, low thermal stability (around 90°C) and high density have limited the PBS products for commercialization. To obtain PBS with superior properties, several types of additives were applied especially for accelerating the crystallization and reducing weight of PBS. The mechanical properties of semicrystalline polymer like PBS is mainly deepened on the crystal structure [5]. The grafted graphene oxide showed a great nucleating effect on PBS crystallization. Differential scanning calorimetry (DSC) test result showed that the melting temperature of PBS was improved by around 14°C with addition of functionalized carbon nanotubes [6]. With graphene oxide, the crystallization temperature was significantly improved together with the spherules size reduction [7]. Under fast scanning calorimetry (FSC), the crystallization at high cooling and heating rates of PBS was significantly improved in the presence of graphene sheet [8]. The significant improvement of

the crystallization was also found in the PBS/cellulose nanocrystals composites [9]. The nonisothermal crystallization result indicated that the silica nanoparticles had a good nucleation effect on PBS crystallization [10].

In recent years, hollow glass microsphere has been involved in the modification of polymers due to its unique structure and its superior characteristics such as light weight, low thermal conductivity and good sound insulation [11 - 16]. HGM has been used in the modification of polymer composite for different applications. In epoxy, the dielectric constant and dielectric loss of the composites decreased simultaneously, with the increased HGM content [12]. The thermal conductivity in polypropylene (PP)/HGM composites linearly decreased with HGM content. Further modification HGM with silane coupling agent was found to have higher thermal conductivity than the unmodified HGM [14]. Moreover, the dielectric constant at 1 MHz was found to decrease with increasing HGM content or reducing HGM density. Adding HGM to epoxy exhibited the strong strain rate effect. The sensitivity factor was found to decrease with increasing of the volume fraction [15]. Thermal conductivity and compressive strength of the epoxy/HGM composites was found to reduce with the addition of HGM as well [16].

Literature review indicated that most of research focused on the observation the electrical properties i.e., dielectric constant, electrical conductivity and mechanical properties of polymer/HGM composites. To extend these studies, this paper focused on studying the effect of particle size, content and the density of HGM on the crystallization behavior, mechanical, morphological and physical properties of PBS.

EXPERIMENTAL

Raw materials

A blown film grade bio-PBS (FZ91PM) was used as a polymer matrix. It was produced by PTT MccBiochem Company Ltd. It has a density of 1.26 g cm^{-3} and a melting point of 115°C. Three types of HGM particles (K25, S60 and S15) were kindly donated from 3M (Thailand) Company Ltd. Further information of the HGM used in the current research is listed in Table 1 and the appearance of the HGM is clearly presented in Fig. 1. S60 shows the smallest particle size and highest true density. The true density of K25, S60 and S15 were 0.248, 0.604, 0.153 g cm^{-3}, while their average particle size (D50) were 55, 30, 55 μm, respectively.

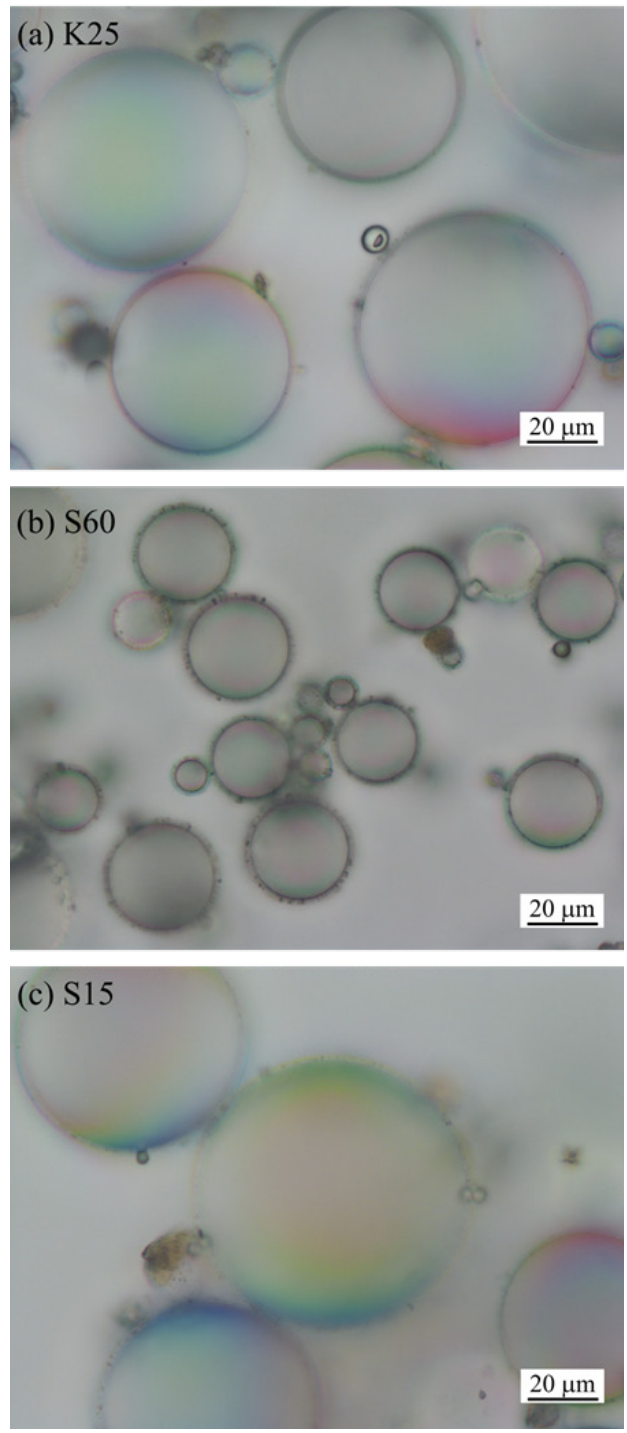

Fig. 1. Visual appearance of HGMs.

Table 1. Properties of HGM used in the current research.

Trade name	True density ($g\ cm^{-3}$)	Average particle size by volume (μm)		
		D10	D50	D90
K25	0.248	25	55	90
S60	0.604	15	30	55
S15	0.153	25	55	90

Preparation of PBS/HGM composites

Firstly, PBS and HGM were dried in a vacuum oven at 65°C for 12 h and then they were dry-mixed with each type of HGM at 2.5, 5.0, 7.5 and 10 wt. %. The dry-blended compositions were compounded by using a twin-screw extruder (Chareon TUT, CTE-D16L512) and then palletized to obtain the PBS/HGM compound pellets. The screw speed of the extruder was 60 rpm and the temperatures along the barrel were 120°C to 155°C. The pelletized PBS/HGM compositions were then fabricated by using an injection molding machine (Chareon TUT, INJ101T) for subsequence testing and characterizations.

Testing and characterizations

The visual appearance of HGMs was observed by using a polarized optical microscope (Nikon LV100POL). The fractured surfaces of the PBS/HGM composites were studied by a scanning electron microscopy (FE-SEM Model, HITACHI-S4700), all specimens were sputter coated with 30 Angstrom of gold prior to examination.

Differential scanning calorimetry analysis was carried out to observe the thermal and crystallization behaviors of PBS composites by using a Perkin Elmer DSC6000 under nitrogen gas atmosphere. The test was performed on 10 mg sample by heating the sample from room temperature to 150°C, and then they were held for 5 min to remove previous thermal history. They were cooled down to 0°C and held for 5 min. Finally, the samples were re-heated to 150°C. All the samples were run at various heating rate of 5, 10 and 30°C min^{-1}. The crystallization and melting thermograms were observed by reporting the glass transition temperature (T_g), melting temperature (T_m) and crystallization temperature (T_c). Further estimation of the degree of crystallinity (X_c) was made following Equation (1) [17,18]:

$$X_c = 100 \times \frac{\Delta H_M}{x_p \times \Delta H^0} \quad (1)$$

where ΔH_m, ΔH_c and x_p are the enthalpy of melting, enthalpy of the crystallization and the weight fraction of the PBS, respectively. ΔH^0 is the heat of fusion, defined as the melting enthalpy of 100 % crystalline PBS, which is 200 J g^{-1} [17, 18].

Tensile properties were performed on a Universal Testing Machine (Instron, 5966) in accordance with ASTM D 638 at a crosshead speed of 5 mm min^{-1}. The gauge length was set at 1 in. The notched Izod impact test was carried out by using a pendulum impact tester (TINIUS OLSEN, 92TD) following the procedure described in ASTM D 256 standard. The density of the PBS/HGM composites was measured by using a densimeter following the Archimedes principle.

RESULTS AND DISCUSSION

Thermal properties

Figs. 2 to 7 illustrate the second heating and cooling DSC thermograms of PBS/HGM composites with various heating rates i.e., 5, 10 and 30°C min^{-1}. Further peaks identification and X_c calculations were made and summarized in Table 2. Figs. 2 to 4 illustrate the crystallization behavior of the PBS composites with various HGM types of K25, S15 and S60, respectively. Overall, the composites showed the identical crystallization behavior at all HGM types and cooling rates. At high heating rates, the T_c shifted to lower temperature by 10°C - 15°C. In this case, the polymer chains did not have enough time to transfer from the melt to the crystals, so crystallization took place at lower temperature [19]. However, there was a slight difference between the HGM types and contents added. This was commonly

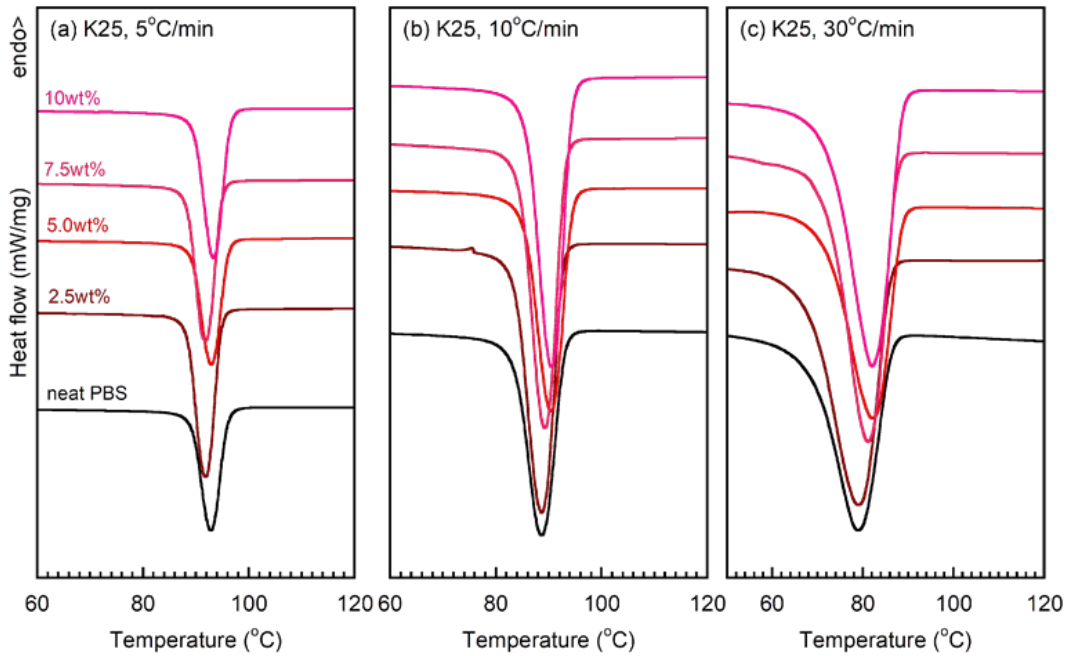

Fig. 2. Crystallization curves of PBS/K25 HGM composites with various heating rates.

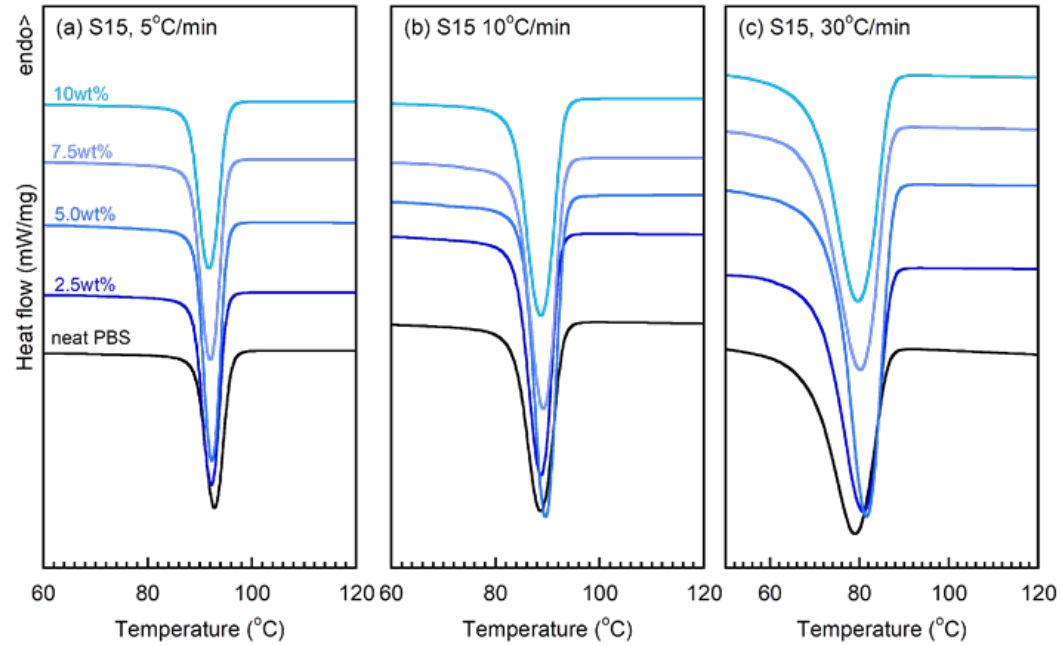

Fig. 3. Crystallization curves of PBS/S15 HGM composites with various heating rates.

observed in the PBS/inorganic fillers composites [11, 20]. In this case, adding high content HGM allowed the agglomeration and limited the nucleation ability.

Figs. 5 to 7 show the melting endotherms of the PBS composites. The samples were all melted at different heating rates from 5 to 30°C min^{-1}. With increasing the heating rate, the height of the samples baseline increased and the T_m shifted to higher position by 4°C - 5°C. The high heating rate accelerated the PBS chain mobility, facilitated the crystallization and shifted the melting point. In Table 2, the area under T_m peaks or ΔH_m was found to increase with the addition of HGM by around 20 J g^{-1} - 40 J g^{-1}. Compared to neat PBS, maximum ΔH_m around 70 J g^{-1} was found when S60 was applied at 10

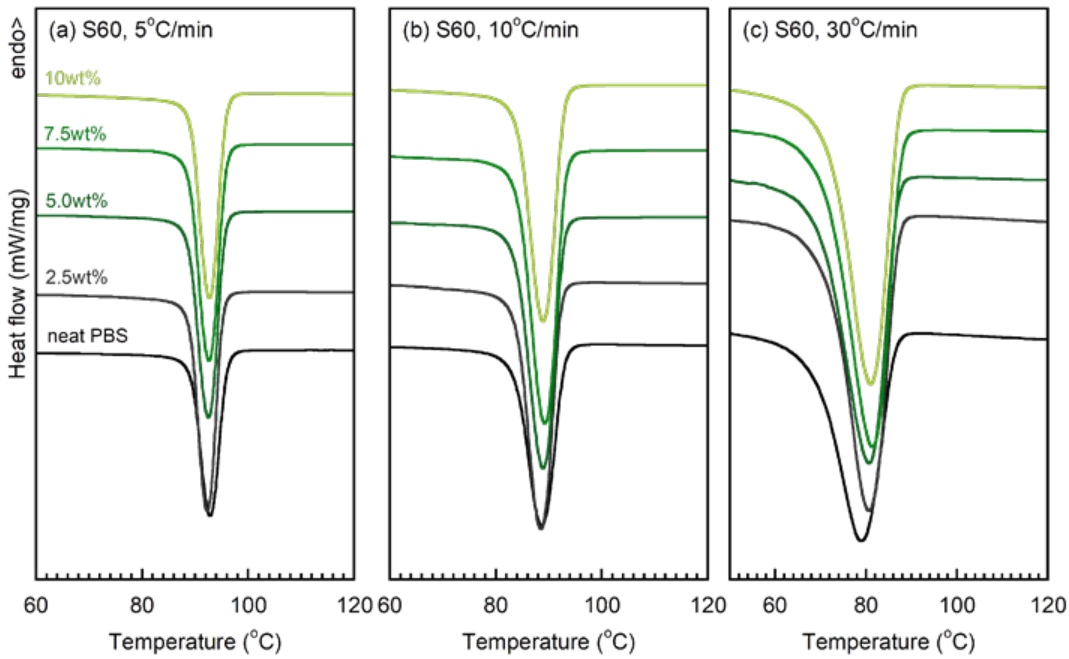

Fig. 4. Crystallization curves of PBS/S60 HGM composites with various heating rates.

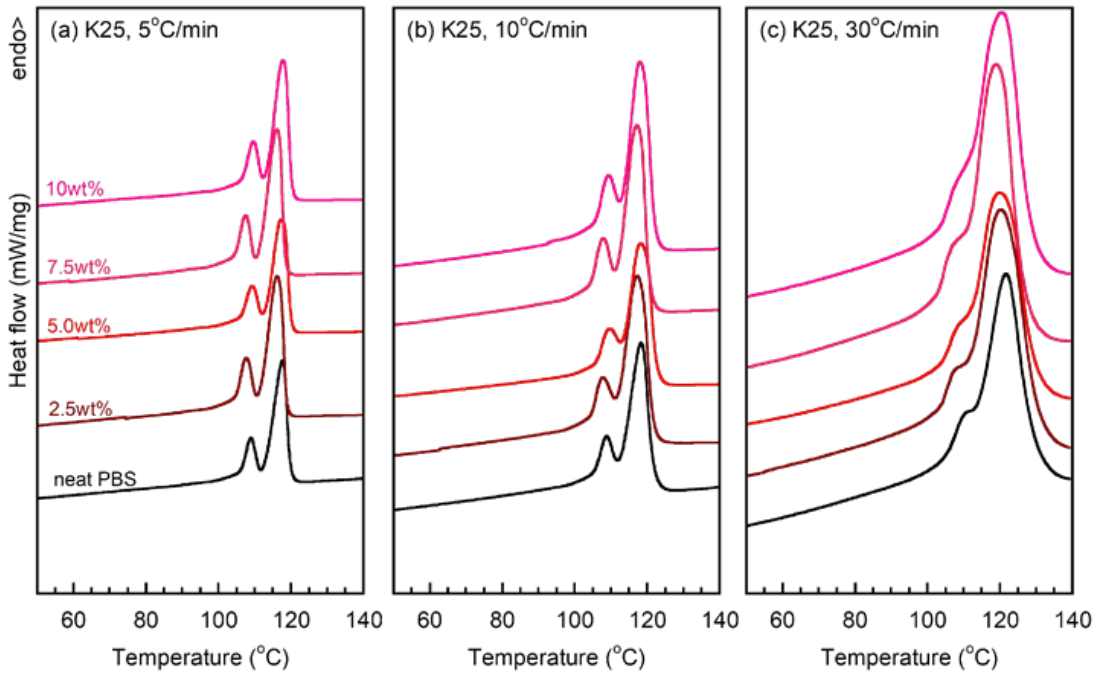

Fig. 5. Second heating thermograms of PBS/K25 HGM composites with various heating rates.

wt. %. This suggested that all the HGMs served as the nucleating agent and increased the crystallization rate of PBS [21, 22]. The degree of crystallinity (X_c) was employed to evaluate the efficiency of HGM on PBS crystal. Also in Table 2, the X_c of neat PBS was varied around 16 % - 18 % due to the heating rate. Adding HGM to PBS significantly played an active role in PBS crystal nucleation. The X_c of PBS increased by at least 1.7 times with the presence of HGM at least 2.5 wt. %. Maximum X_c of 39.18 % were observed when S60 was added at 10 wt. %. In comparison, there was a slight difference of the X_c with various HGM contents. This was believed to be the resulted of the agglomerated HGM, which possibly brought them less effective in crystal nucleation [11].

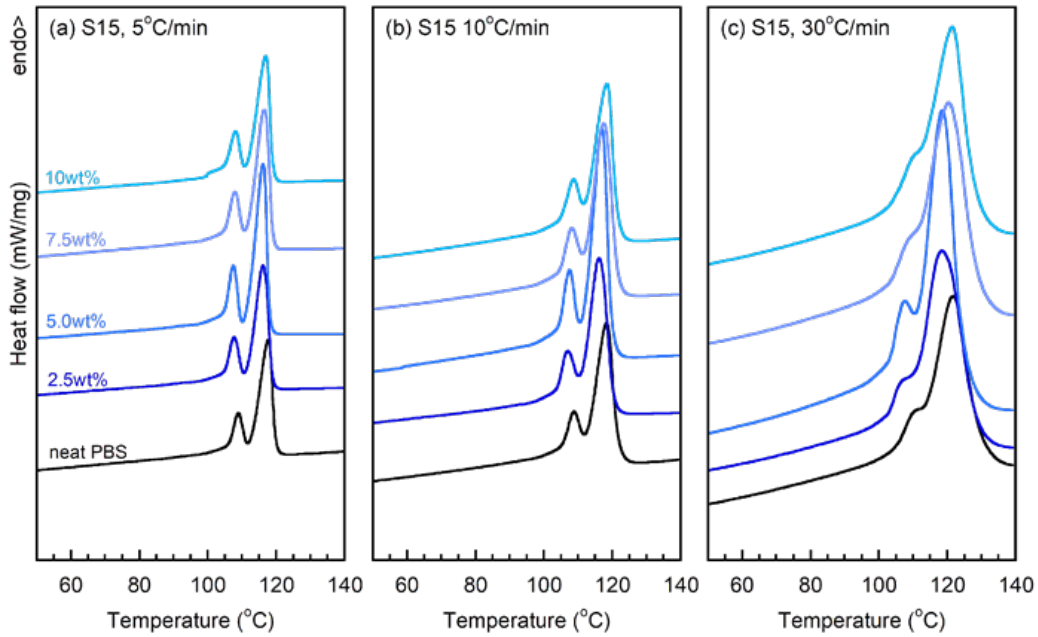

Fig. 6. Second heating thermograms of PBS/S15 HGM composites with various heating rates.

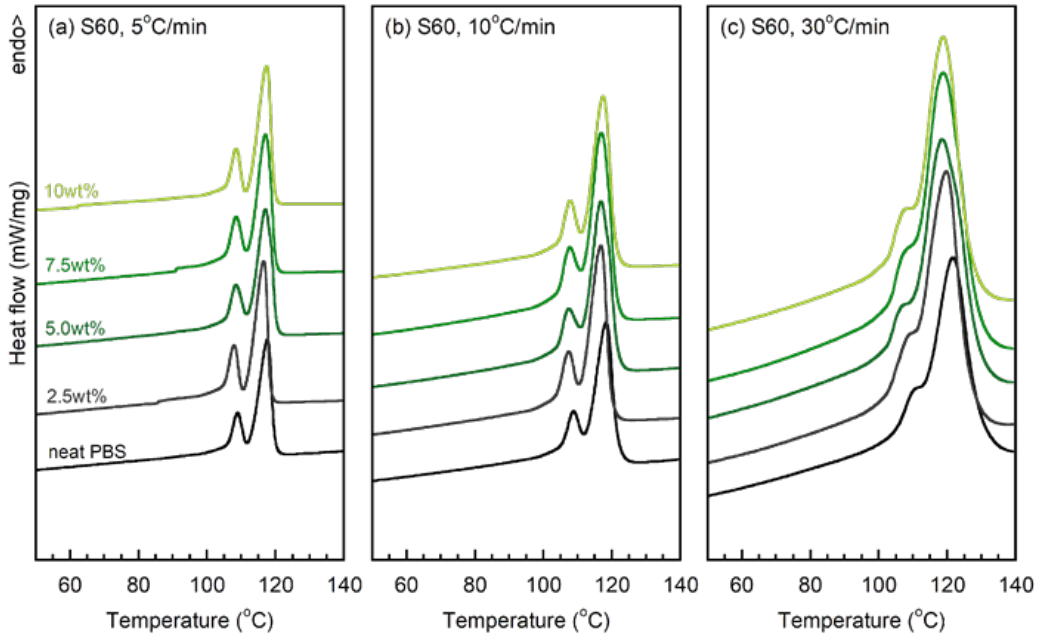

Fig. 7. Second heating thermograms of PBS/S60 HGM composites with various heating rates.

Microscopic observation and mechanical properties

Fig. 8 illustrates the SEM micrograph of the PBS modified with S15, S60 and K25 HGM. Based on the data in Table 1, S60 had the highest density. The S15 and K25 had lower density, which made them much more brittle and less tolerance to the pressure and shearing force [23]. In Fig. 8(b - m), HGB was found to uniformly disperse in PBS matrix only at 2.5 wt. % and 5.0 wt. %, but it seemed agglomerated at 7.5 wt. % and 10 wt. %. This agglomerated HGM particles were difficult to disperse as separated particles in steady shear flow, which could be found in the conventional extruder [24]. Moreover, there are some pulled-out HGM particles at all concentrations, which indicated the poor interfacial adhesion between PBS and HGM. The broken HGM were generally observed at 7.5 wt. % and 10 wt. % for PBS with S15 and K25. For S60,

Table 2. Thermal properties of PBS/HGM composites,

PBS and HGM type	HGM content (wt. %)	Heating rate (°C min^{-1})	T_c (°C)	ΔH_c (J g^{-1})	T_m (°C)	ΔH_m (J g^{-1})	X_c (%)
Neat PBS	0	5	92.84	42.56	117.6	36.58	18.29
		10	88.62	40.88	118.2	35.26	17.63
		30	79.19	39.17	121.9	33.27	16.64
K25	2.5	5	91.89	72.27	116.1	65.97	33.83
		10	86.66	65.22	117.2	65.28	33.48
		30	79.36	65.61	120.4	64.38	33.02
	5.0	5	92.91	54.64	117.3	57.68	30.36
		10	90.43	54.91	118.2	57.67	30.35
		30	82.12	52.15	120.0	52.68	27.73
	7.5	5	91.87	61.07	116.1	64.37	34.79
		10	89.35	61.39	117.0	61.15	33.05
		30	81.35	60.04	118.8	59.93	32.39
	10	5	93.36	55.42	117.8	62.77	34.87
		10	90.69	64.77	118.0	60.75	33.75
		30	82.29	61.89	120.4	58.66	32.59
S60	2.5	5	92.29	61.01	116.5	58.55	30.03
		10	88.52	60.15	116.7	60.00	30.77
		30	80.80	59.95	119.8	51.72	26.52
	5.0	5	92.52	59.76	117.1	59.19	31.15
		10	89.03	61.84	116.8	59.34	31.23
		30	80.83	59.45	118.3	56.27	29.62
	7.5	5	92.70	58.45	117.1	58.01	31.36
		10	89.38	64.25	116.8	62.33	33.69
		30	83.73	58.29	118.8	57.09	30.86
	10	5	92.69	58.67	117.4	70.53	39.18
		10	89.00	60.03	117.3	60.07	33.37
		30	81.32	61.35	118.8	57.03	31.68
S15	2.5	5	91.75	53.81	117.0	52.67	27.01
		10	88.48	55.92	118.3	52.67	27.01
		30	79.84	54.42	121.4	49.29	25.28
	5.0	5	92.40	64.87	116.1	70.32	37.01
		10	89.58	70.74	116.8	66.94	35.23
		30	81.93	64.97	118.2	61.73	32.49
	7.5	5	92.04	57.26	116.6	59.43	32.12
		10	89.00	57.46	117.5	55.32	29.90
		30	80.27	54.24	120.4	51.34	27.75
	10	5	91.75	54.38	117.0	54.55	30.31
		10	88.48	55.40	118.3	52.47	29.15
		30	79.84	54.37	121.3	50.11	27.84

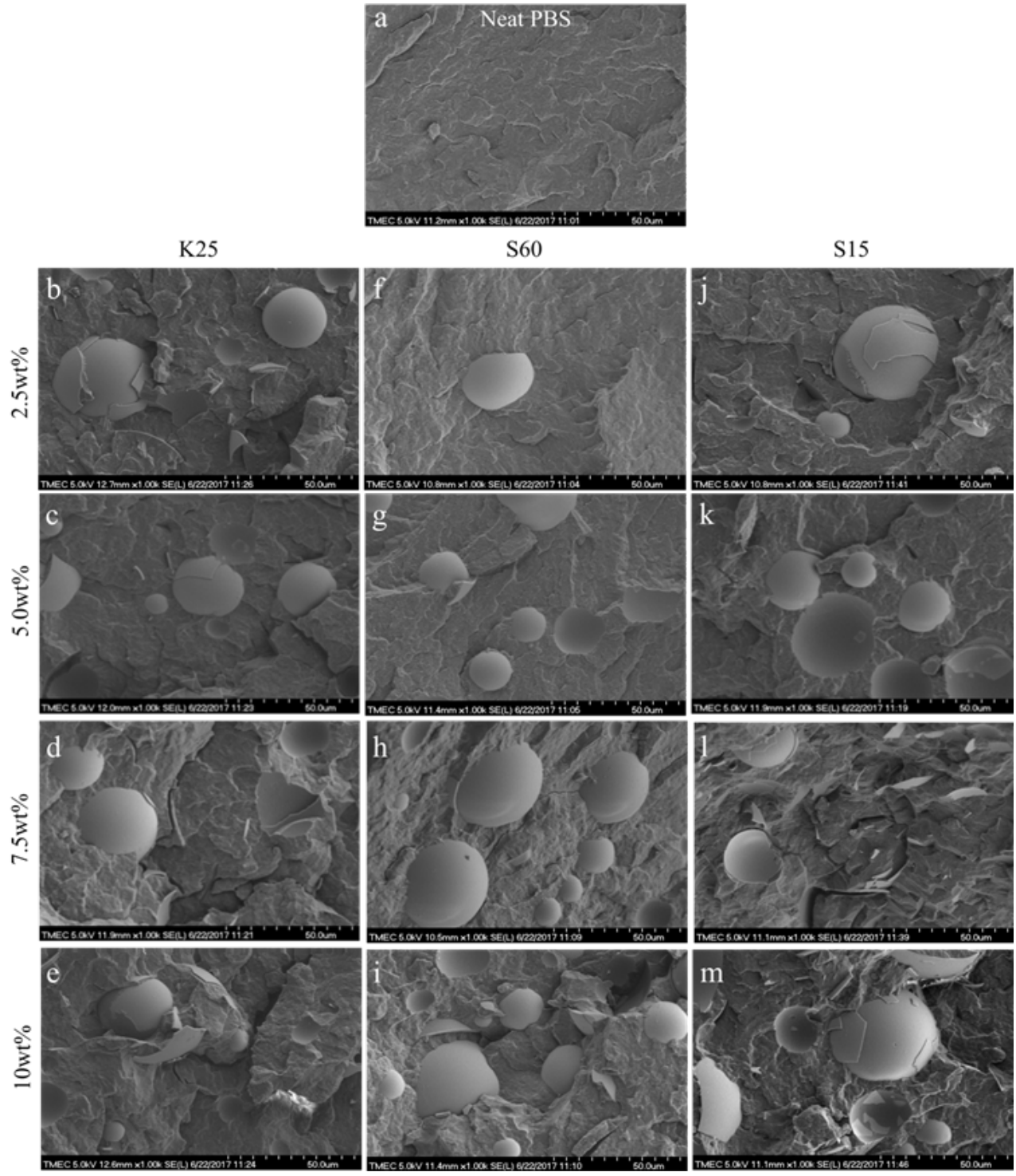

Fig. 8. SEM micrograph of PBS composites with various HGM types.

it did only at 10 wt. %. These HGM fractures were possibly due to i) the high shearing force and high pressure of twin-screw extrusion and injection molding processes and ii) the propagation of the crack during the fracture process of the SEM sample preparation. This correlated to the data presented in Table 1, which informed that the K25 and S15 HGM have lower density, larger particle size and thinner glass wall than S60, which made them less durable to high shearing force, high pressure and crack propagation. The poor interfacial bonding between

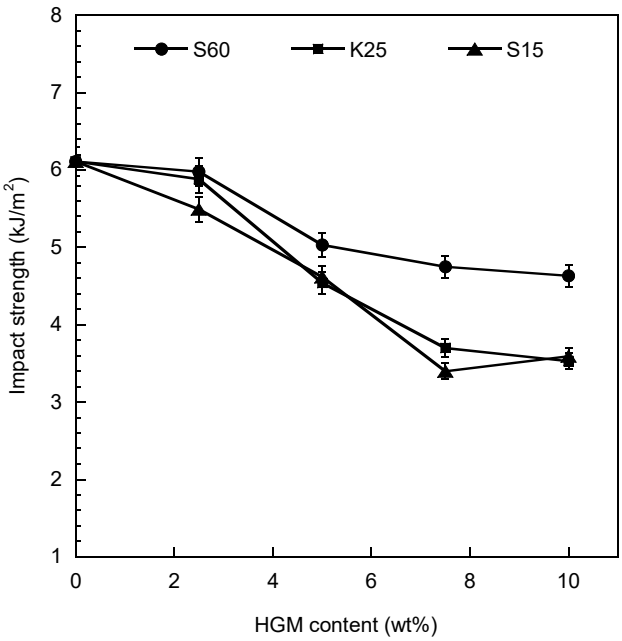

Fig. 9. Impact strength of PBS composites with various HGM types.

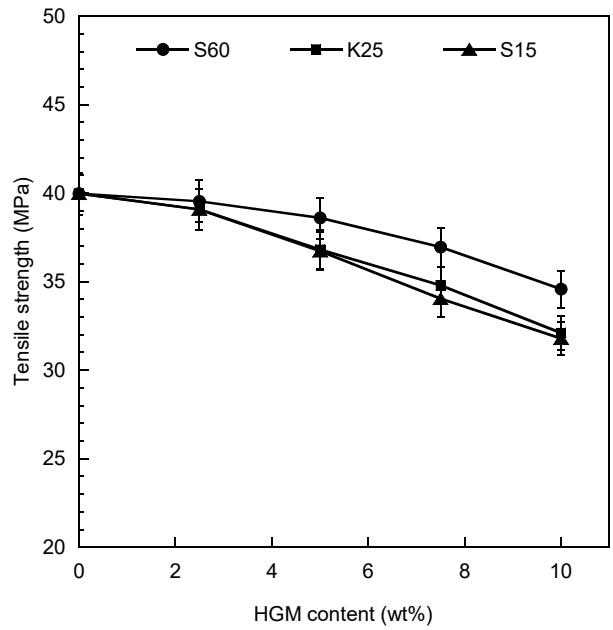

Fig. 10. Tensile strength of PBS composites with various HGM types.

the polymer matrices and some fractured HGM particles were also found in the PBS/HGM [11] and thermoplastic polyurethane composites [24].

The addition of HGM brought the brittleness to PBS at all concentrations and HGM types (Fig. 9). However, S60 exhibited higher impact strength than that of K25 and S15. These reductions were mainly due to the poor interfacial bonding between PBS and HGM, and the brittle nature of HGM which easily fracture during crack propagation. In Fig. 10, the tensile strength slightly decreased with increasing HGM content especially at 7.5 wt. % and 10 wt. %. These were due to i) some pulled-out HGM particles, ii) the broken HGM particles and iii) theagglomeration of the HGM particles, which limited the filler-matrix stress transfer [24]. In comparison, S15 and K25 exhibited lower tensile strength than that of S60. This was mainly caused by the broken HGM mostly observed in S15 and K25. This directly decreased the effectiveness of reinforcement [24]. The elongation at break (Fig. 11) was significantly reduced from around 18 % to less than 5 % at all compositions. Reduction of the elongation at break was caused by the restriction of PBS chain entanglement induced by HGM [25]. These reductions of all the impact strength, tensile strength and the elongation at break were previously reported by many researchers. Both the tensile strength and the elongation at break of thermoplastic polyurethane/HGM composites reduced with increasing the HGM loading [24]. The impact strength of the PBS/HGM composites

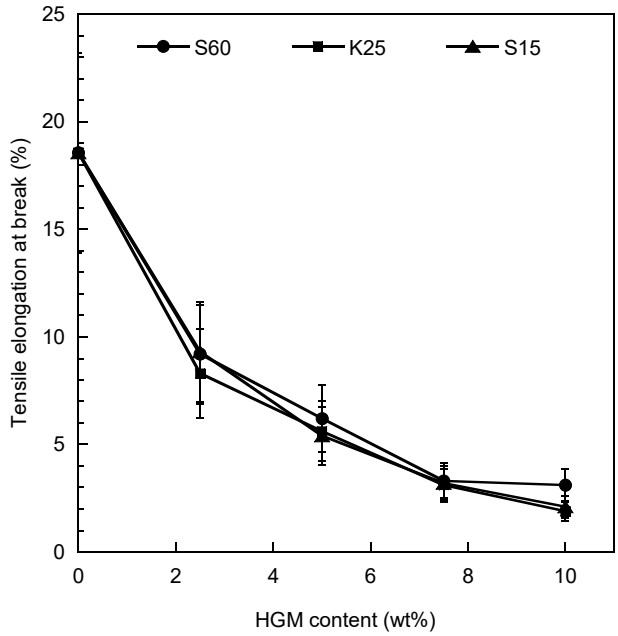

Fig. 11 Tensile elongation at break of PBS composites with various HGM types.

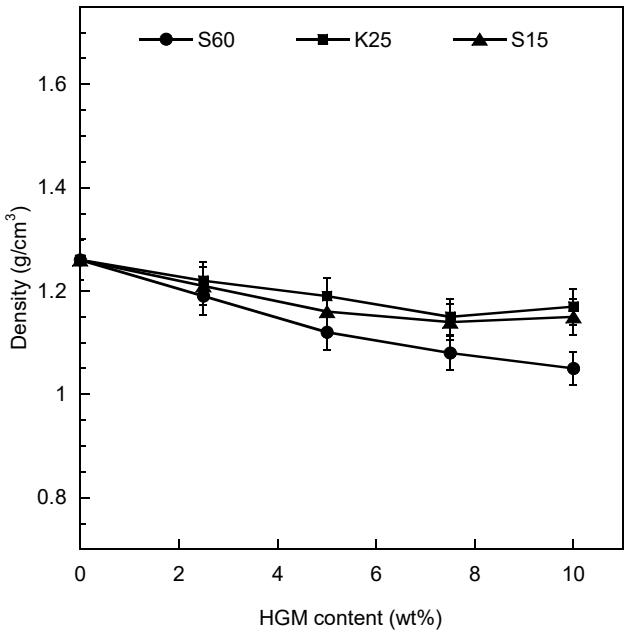

Fig. 12. Density of PBS composites with various HGM types.

was lower than neat PBS when HGM was added at 10 wt. %. However, adding more HGM up to 15 wt. % was found to increase the impact strength due to complete stress transfer path [11].

Density

The density of neat PBS and PBS/HGM composites measured by a densimeter is graphically presented in Fig. 12. Overall, the density of the composite decreased with the increase of HGM content. The lowest density of 1.05 g cm^{-3} was observed in the PBS with 10 wt. % S60. For S15 and K15, the densities were higher than S60. This was mainly due to the broken HGM as evidenced in SEM micrographs.This density reduction was in agreement with other polymers/HGM composites [11,15].

CONCLUSIONS

Three types of HGMs were employed as nucleating agents in PBS namely K25, S60 and S15. Overall, the smaller HGM particles tended to exhibite better mechanical, thermal properties and density reduction than the larger ones. Thermal test results indicated that the X_c of PBS increased with the addition of HGM by at least 1.7 times. However, there was a slight difference in the crystallization behavior among the HGM types and contents studied. SEM micrographs showed some agglomerations and broken particles at high HGM contents. Moreover, there are some pulled-out HGM particles at all concentrations. These restricted the HGM-matrix stress transfer and reduced the tensile strength. The density of PBS/HGM composites were all reduced with the concentration. The lowest density of 1.05 g cm^{-3} was observed in the PBS with 10 wt. % S60. For S15 and K15, the densities were both higher than S60.

Acknowledgements

The authors would like to acknowledge the research grant supported by Srinakharinwirot University (Contract no. 006/2561). Thanks are extended to Mr.Kittisak Phromsuk, Mr.Sarit Sukwattanajaroon and Mr.Rittiporn Aroonrasmeruang for the preliminary study of this research.

REFERENCES

1. N. Petchwattana, P. Naknaen, Utilization of thymol as an antimicrobial agent for biodegradable poly(butylene succinate),Mater. Chem. Phys., 163,2015, 369-375.
2. K. Thakur, S. Kalia, Enzymatic modification of ramie fibers and its influence on the performance of ramie-poly(butylene succinate) biocomposites, Int. J.Plast. Technol., 21, 1, 2017, 209-226.
3. Y.F. Shih, T.Y. Wang, R.J. Jeng, J.Y. Wu, C.C. Teng, Biodegradable nanocomposites based on poly(butylene succinate)/organoclay, J.Polym. Environ.,15, 2, 2007, 151-158.
4. X. Wang, H. Yang, L. Song, Y. Hu, W. Xing, H.Lu, Morphology, mechanical and thermal properties of graphene-reinforced poly(butylene succinate) nanocomposites, Compos. Sci. Technol.,72, 1, 2011,1-6.
5. T.R. Panthani, F.S. Bates, Crystallization and mechanical properties of poly(l-lactide)-based rubbery/semicrystalline multiblock copolymers, Macromolecules, 48, 13, 2015, 4529-4540.
6. R.T. Zeng, W. Hu, M. Wang, S.D. Zhang, J.B. Zeng, Morphology, rheological and crystallization behavior in non-covalently functionalized carbon nanotube

reinforced poly(butylene succinate) nanocomposites with low percolation threshold, Polym. Test, 50, 2016, 182-190.
7. T.X. Jin, C. Liu, M. Zhou, S.G. Chai, F. Chen, Q.Fu, Crystallization, mechanical performance and hydrolytic degradation of poly(butylene succinate)/ graphene oxide nanocomposites obtained via in situ polymerization, Compos. Part A-Appl. S., 68, 2015, 193-201.
8. N. Bosq, N. Guigo, D. Aht-Ong, N. Sbirrazzuoli, Crystallization of poly(butylene succinate) on rapid cooling and heating: Toward enhanced nucleation by graphene nanosheets, J. Phys. Chem. C, 121, 21, 2017, 11915-11925.
9. Y.D. Li, Q.Q. Fu, M. Wang, J.B. Zeng, Morphology, crystallization and rheological behavior in poly(butylene succinate)/cellulose nanocrystal nanocomposites fabricated by solution coagulation, Carbohydr. Polym., 164, 2017, 75-82.
10. J. Bian, L. Han, X. Wang, X. Wen, C. Han, S. Wang, L. Dong, Nonisothermal crystallization behavior and mechanical properties of poly(butylene succinate)/ silica nanocomposites, J. Appl. Polym. Sci.,116, 2, 2010, 902-912.
11. J. Li, X. Luo, X. Lin, Preparation and characterization of hollow glass microsphere reinforced poly(butylene succinate) composites, Mater. Design., 46, 2013, 902-909.
12. K.C. Yung, B.L. Zhu, T.M. Yue, C.S. Xie, Preparation and properties of hollow glass microsphere-filled epoxy-matrix composites, Compos. Sci. Technol., 69, 2, 2009, 260-264.
13. J.Z. Liang,Estimation of thermal conductivity for polypropylene/hollow glass bead composites, Compos. Part B Eng., 56, 2014, 431-434.
14. B.L. Zhu, H. Zheng, J. Wang, J. Ma, J. Wu, R.Wu,Tailoring of thermal and dielectric properties of LDPE-matrix composites by the volume fraction, density, and surface modification of hollow glass microsphere filler, Compos. Part B Eng., 58, 2014, 91-102.
15. X. Zhang, P. Wang, Y. Zhou, X. Li, E.H. Yang, T.X. Yu, J. Yang, The effect of strain rate and filler volume fraction on the mechanical properties of hollow glass microsphere modified polymer, Compos. Part B Eng.,101, 2016, 53-63.
16. Y. Qiao, X. Wang, X. Zhang, Z.Xing, Thermal conductivity and compressive properties of hollow glass microsphere filled epoxy–matrix composites, J. Reinf. Plast. Compos., 34, 17, 2015, 1413-1421.
17. I.N. Georgousopoulou, S. Vouyiouka, P. Dole, C.D. Papaspyrides, Thermo-mechanical degradation and stabilization of poly(butylene succinate), Polym. Degrad. Stab., 128, 2016, 182-192.
18. Y. Zhang, C. Yu, P.K. Chu, F. Lv, C. Zhang, J. Ji, R. Zhang, H.Wang, Mechanical and thermal properties of basalt fiber reinforced poly(butylene succinate) composites, Mater. Chem. Phys.,133, 2012, 845-849.
19. C. Li, Q. Dou,Non-isothermal crystallization kinetics and spherulitic morphology of nucleated poly(lactic acid): Effect of dilithiumhexahydrophthalate as a novel nucleating agent, Thermochim. Acta, 594, 2014, 31-38.
20. W.G. Liu, X.C. Zhang, H.Y. Li, Z. Liu, Effect of surface modification with 3-aminopropyltriethyloxy silane on mechanical and crystallization performances of ZnO/poly(butylenesuccinate) composites, Compos. Part B Eng., 43, 2012, 2209-2216.
21. F.B. Ali, R. Mohan, Thermal, mechanical, and rheological properties of biodegradable polybutylene succinate/carbon nanotubes nanocomposites, Polym. Composite, 31, 8, 2010, 1309-1314.
22. N. Petchwattana, P. Naknaen, J. Sanetuntikul, B. Na rupai,Crystallisation behaviour and transparency of poly(lactic acid) nucleated with dimethylbenzylidene sorbitol, Plast. Rubber Compos., 47, 4, 2018,147-155.
23. Y. Hua, R. Mei, Z. An, J. Zhang, Silicon rubber/ hollow glass microsphere composites: Influence of broken hollow glass microsphere on mechanical and thermal insulation property, Compos. Sci. Technol., 79, 2013, 64-69.
24. X. Lu, J. Qu, J.Huang, Mechanical, thermal and rheological properties of hollow glass microsphere filled thermoplastic polyurethane composites blended by normal vane extruder, Plast. Rubber Compos., 44, 8, 2015, 306-313
25. N. Petchwattana, P. Sriromruen, J. Sanetuntikul, B. Naruepai, Wood plastic composites prepared from biodegradable poly(butylene succinate) and Burma padauk sawdust (Pterocarpus macrocarpus): Water absorption kinetics and sunlight exposure investigations, J. Bionic Eng.,14, 4, 2017,781-790.